

Evaluating Quantumness, Efficiency and Cost of Quantum Random Number Generators via Photon Statistics

Goutam Paul,^{1,*} Nirupam Basak,^{1,†} and Soumya Das^{2,‡}

¹*Cryptography and Security Research Unit, Indian Statistical Institute, Kolkata 700108, India*

²*Dept. of Math. and Comp. Sci., Eindhoven University of Technology, Netherlands*

Despite the availability of commercial QRNG devices, distinguishing between PRNG and QRNG outputs computationally remains challenging. This paper presents two significant contributions from the perspectives of QRNG manufacturers and users. For manufacturers, the conventional method of assessing the quantumness of single-photon-based QRNGs through mean and variance comparisons of photon counts is statistically unreliable due to finite sample sizes. Given the sub-Poissonian statistics of single photons, confirming the underlying distribution is crucial for validating a QRNG's quantumness. We propose a more efficient two-fold statistical approach to ensure the quantumness of optical sources with the desired confidence level. Additionally, we demonstrate that the output of QRNGs from exponential and uniform distributions exhibit similarity under device noise, deriving corresponding photon statistics and conditions for ϵ -randomness.

From the user's perspective, the fundamental parameters of a QRNG are quantumness (security), efficiency (randomness and random number generation rate), and cost. Our analysis reveals that these parameters depend on three factors, expected photon count per unit time, external reference cycle duration, and detection efficiency. A lower expected photon count enhances security but increases cost and decreases the generation rate. A shorter external reference cycle boosts security but must exceed a minimum threshold to minimize timing errors, with minor impacts on cost and rate. Lower detection efficiency enhances security and lowers cost but reduces the generation rate. Finally, to validate our results, we perform statistical tests like NIST, Dieharder, AIS-31, ENT etc. over the data simulated with different values of the above parameters. Our findings can empower manufacturers to customize QRNGs to meet user needs effectively.

Keywords: Photon Statistics, Randomness, Quantumness, QRNG

I. INTRODUCTION

Random numbers have important roles in numerous applications, including computational methods like Monte Carlo simulations and programming [1, 2], testing principles of physics and chemistry [3], as well as in the expansive realm of cryptography for creating cryptographic codes or concealing messages [4, 5], extending to commercial uses such as slot machines and lottery games [6, 7]. In cryptography, randomness is a key input to ensure security in communication. Classical pseudorandom number generators (PRNG) cannot guarantee communication security due to their deterministic generation process. On the contrary, the randomness of a true random number generator (TRNG) is rooted in some physical entropy source [8, 9]. A quantum random number generator (QRNG) uses the quantum particles and the principles of quantum physics [10] to produce random numbers.

Statistically, it is not feasible to distinguish between a PRNG and a QRNG just by analyzing their outputs. Statistical tests like NIST [11], Dieharder [12], AIS-31 [13], ENT [14] etc. are available to test the randomness of a random number generator (RNG). However, from the

results of these tests, it is not possible to say whether an RNG is quantum or not. So a pertinent question arises:

Q1: *How do we test whether an alleged QRNG is truly quantum or not?*

Different technologies, including photon arrival time [15–22], tunneling [23, 24], fluctuation [25–30], phase noise [31–37], etc. have been proposed to produce QRNGs [38, 39]. Several manufacturers such as ID Quantique [40], Qtools [41], QNuLabs [42], Quintessence-Labs [43], Mars Innovation [44], Quantum Computing Inc. [45], Quside [46], QuantumCTek [47] are producing QRNGs following these technologies. These QRNGs are commercially available as off-the-shelf black-box devices. As the photon arrival-time-based QRNGs are the most general and most of the companies follow this approach, in this work we try to answer the Q1 with respect to this type of QRNGs.

In most of the analyses [48–51] of the photon arrival-time-based QRNGs, the photon statistics have been discussed either by comparing the mean and variance of the sample distribution or using the negativity of the Mandel parameter [52]. For example, Alléaume et al. [53] discussed photon statistics of photon sources using the Mandel parameter given by [52, Eq. (11a)]. They calculated values of the Mandel parameter from observed photon count timestamps and concluded that negative values of the Mandel parameter, which indicates sub-Poissonian statistics, signify non-classical photon statistics for photon sources. Although analytically it is true, a negative value of the Mandel parameter for experimental data may

* goutam.k.paul@gmail.com

† nirupambasak2020@iitkalumni.org

‡ s.das2@tue.nl

not always indicate sub-Poissonian statistics. For example, a finite number of photon count timestamps from coherent light that actually follows Poissonian distribution may result in a negative value of the Mandel parameter. This happens because the mean and the variance of a sample with a finite size may not always be the same as the mean and the variance of the underlying distribution. Therefore, calculating the exact value of any parameter from a sample of finite size is not enough to decide the underlying nature of the distribution.

Another approach to test the quantumness of light is to experimentally observe photon antibunching [54]. However, although a stream of antibunched photons indicates the non-classical nature of light, the converse is not necessarily true. In other words, non-classical light can sometimes be observed as bunched photons [55, 56]. We explain this in more detail in Appendix A. This approach also consists of an equality criteria similar to above photon statistics case. Therefore this is also not enough to decide photon antibunching.

On the other hand, a single-photon source ensures the quantumness of a QRNG [54, 56]. However, generating single photons are experimentally challenging task [57, 58]. Various experimental methods [59–66] have been explored to produce single photons. Existing time-bin-based QRNG models utilize coherent photon sources in conjunction with attenuators to produce random numbers from exponential [17–19] or uniform [15] distributions if the underlying optical devices perform ideally and the source generates perfectly single photon. But, in practice, this is not the case. Therefore, it is important to explore the photon statistics in practical scenarios.

Also, all of the QRNGs require some classical post-processing using deterministic functions. These post-processings use a classical source of randomness to increase randomness in the raw data generated by the QRNGs. Side-channel attacks [67–69] can also be performed in this post-processing step to gather information about the random number. Therefore, the amount of classical post-processing should be minimal to ensure the randomness from the quantum source in the final outputs and reduce the possibility of side-channel attacks on classical post-processing. To achieve this, the raw output number (before classical post-processing) generated by QRNG should be as close to uniform random as possible. As all the practical devices are prone to error, this raises an important question:

Q2: *How to increase the randomness from the quantum source in the presence of device errors?*

Besides quantumness and randomness, the random number generation rate and the cost of the QRNG are also important parameters from the user’s perspective. The trade-off between the randomness from the quantum source, the random number generation rate and the cost of the QRNG depends on the users’ requirements. For example, in the case of secure communication, the randomness from the quantum source should have the highest priority, and also the generation rate should be

high. On the other hand, in token generation or lottery games, a low rate of random number generation would be sufficient. Therefore, to fulfill the user’s requirement, the answers to the following questions are required.

Q3: *How to choose the optical parameters (a) the photon numbers in unit time, (b) the time cycle and (c) the detection efficiency of a QRNG depending on the user’s requirements?*

In this article, we aim to evaluate the quantumness of photon arrival-time-based QRNG from the manufacturer’s perspective as answers to Q1 and Q2 and randomness, random number generation rate, and cost from the user’s perspective as the answer to Q3. For the manufacturer, we first address the validation of quantum sources using photon counting statistics. Considering that the sample data for the number of photons within a fixed time is available, we suggest a two-fold statistical method to verify whether the source of the sample is quantum or not, overcoming the limitations of the existing approaches discussed above. The method consists of interval estimation and hypothesis testing, to ensure sub- or super-Poissonian distribution up to a desired confidence level.

As another contribution, also from the manufacturer’s perspective, we derive the photon statistics for two-photon arrival-time-based QRNGs in practical scenarios. These photon statistics for QRNGs can be considered as a measure of randomness from quantum sources for photon arrival-time-based QRNGs. Depending on this measure, a suitable post-processing algorithm can be chosen to retain the maximum amount of randomness from the quantum source. For the practical scenario, we consider power instability as the error of the source and the attenuators and detection inefficiency as the error of a single photon detector (SPD).

From the user’s perspective, we see that the maximum randomness from the quantum source may not be achieved due to some practical constraints related to the random number generation rate, the timing error in registering the photon detection time and the cost of the QRNG. In particular, we show the following.

- If the expected number of photons within a unit of time is small, the randomness from the quantum source would be high. However, it would increase the cost of the QRNG, and also, it would reduce the random number generation rate.
- Although a small external reference cycle of the QRNG increases the randomness from the quantum source, to minimize the timing error, it should be higher than a specific value. This reference cycle does not have much effect on the cost or random number generation rate of the QRNG.
- A detector with less efficiency increases the randomness from the quantum source and also reduces the cost of the QRNG. However, it also reduces the random number generation rate.

Finally, we simulated random numbers depending on photon statistics we have derived, and performed statistical tests like NIST [11], Dieharder [12], AIS-31 [13] and ENT [14] on those random numbers. We show that these statistical tests support our theoretical deduction regarding randomness from quantum sources.

This paper is structured as follows. In Section II we perform some preliminary discussion about photon statistics, some statistical tools used in this work and common randomness testing suites. In Section III and IV we revisit single-photon-based QRNGs and coherent pulse-based QRNGs respectively and mention their weakness in present days. Section V reveals our two-fold proposal to check the quantumness of a quantum device as an answer to Q1. Detailed discussion on coherent pulse-based QRNGs has been performed in Section VI to answer Q2. Section VII answers Q3 by separately analyzing the effects of the parameters mentioned in that question. Results from different randomness testing suites for our simulated random numbers based on the analysis of Section VI are given in Section VIII. Finally, in Section IX we conclude our work.

II. PRELIMINARIES

In this section we first discuss photon statistics. We also discuss how these photon statistics distinguish quantum light from classical light. After that, we mention some statistical tools used in this work. Then we briefly discuss common randomness testing suites for testing the randomness of random numbers

A. Photon Statistics

Photon detection and counting is an important part of QRNG which is further used in other practical applications such as quantum cryptography and quantum communication protocols [4, 5]. In general, photon-based QRNGs generate random numbers by detecting single photons. Therefore, the photon-counting statistics have an important role in determining whether the light falls in the quantum regime or not.

The distribution of the photon-counting statistics can be divided into three classes [56]:

- (i) sub-Poissonian, i.e., the distribution variance is less than the mean,
- (ii) Poissonian, i.e., the distribution variance is the same as the mean, and
- (iii) super-Poissonian, i.e., the distribution variance is greater than the mean.

Classical wave theory of light follows Poissonian and super-Poissonian statistics [56]. On the other hand, the sub-Poissonian nature of a photon source is a clear indication of its quantumness [70, 71].

Let us consider a probability distribution given by,

$$P(n) = \begin{cases} \frac{e^{-\alpha\mu}(\alpha\mu)^{\alpha n}}{(\alpha n)!}, & n = 0, 1, 2, \dots \text{ if } \alpha n \text{ is integer,} \\ 0, & \text{otherwise} \end{cases} \quad (1)$$

for some positive real numbers μ, α . Then the mean would be μ and variance would be $\frac{\mu}{\alpha}$. Therefore, this denotes a sub-Poissonian, Poissonian, or super-Poissonian distribution for $\alpha > 1, \alpha = 1, \alpha < 1$ respectively.

Thermal light follows Bose-Einstein distribution [56], given by

$$P(n) = \frac{1}{\mu + 1} \left(\frac{\mu}{\mu + 1} \right)^n. \quad (2)$$

The mean of this distribution is given by μ , and the variance is $\mu + \mu^2 > \mu$. Therefore, this is a super-Poissonian distribution and hence thermal light is an example of classical light.

Next consider a perfect single-photon source that emits photons maintaining equal time interval, Δt between two consecutive photons. Then the photon count within time T would be the integer $\mu = \lfloor \frac{T}{\Delta t} \rfloor$. In this case, the mean photon count is given by μ , but the variance is $0 < \mu$. Therefore, this is an example of non-classical or quantum light.

A coherent photon source produces coherent states which can be represented as a superposition of Fock states by

$$|\psi_\alpha\rangle = e^{-\frac{|\alpha|^2}{2}} \sum_{n=0}^{\infty} \frac{\alpha^n (\hat{a}^\dagger)^n}{\sqrt{n!}} |0\rangle, \quad (3)$$

where α is a complex number and \hat{a}^\dagger is the creation operator. The mean photon number corresponding to this state is given by $|\alpha|^2$. This state can be approximated as a single-photon state with high attenuation. The probability of n photons within T time follows Poisson distribution [72] given by

$$P(n, T) = \frac{e^{-\mu T} (\mu T)^n}{n!}, \quad (4)$$

where μ is the mean number of photons per unit time. It can be shown that for this distribution, the variance of the number of photons per unit time is also μ .

B. Statistical Tools

1. Interval Estimation

In statistics, an interval (a, b) is called the *confidence interval* for a distribution parameter Θ , if $P(A < \Theta < B) = 1 - \epsilon$ for some predefined $\epsilon \in (0, 1)$, where A, B are the random variables corresponding to the *statistics* a, b (they are functions of sample values) respectively. The quantity $1 - \epsilon$ is called *confidence level* of the interval.

The procedure of finding the confidence interval for the parameter Θ is called *interval estimation*. A statistic a is called an *unbiased estimate* of an unknown parameter Θ if the expectation $\langle A \rangle = \Theta$. A statistic a is called a *consistent estimate* of a parameter Θ if for every real $\epsilon > 0$, $\lim_{n \rightarrow \infty} P(|A - \Theta| \geq \epsilon) = 0$, where n is the sample size.

2. Hypothesis Testing

In statistics, a *hypothesis* is a statement or an assumption about a population distribution. This may be right or wrong. *Hypothesis testing* is a procedure to decide whether a statistical hypothesis, called the *null hypothesis* H_0 , should be rejected or not. A *critical region* or *rejection region* of hypothesis testing is a specific region of test statistic values, for which the null hypothesis is rejected. The *test statistic* for a hypothesis test is a function of the testing sample [73]. A hypothesis test is called *one-tailed* if the critical region appears only at one tail of the reference distribution of the test statistic. On the other hand, it is called a *two-tailed* test, if the critical regions appear at both tails of the above distribution.

During hypothesis testing, two types of error may occur. *Type I error* occurs when H_0 is rejected given that it is true. *Type II error* occurs when H_0 is accepted given that it is false. Let α and β be the probabilities of Type I and Type II errors respectively. The value α denotes the area of the critical region and is also called the *significance level*. The value $1 - \beta$, that is, the probability that H_0 is rejected given that it is false, is also called the *power of a test*.

A hypothesis test starts with two hypotheses: the null hypothesis (H_0) and the alternative hypothesis (H_a). Depending on the significance level α , the critical region is decided. The acceptance or rejection decision of H_0 is based on what is called the *p-value* of the test statistic. It is defined as $P(|X| > |x|)$, where X is a random variable, whose distribution is the reference distribution of the test statistic of a hypothesis test, and x is the observed value of this statistic [74, 75]. When the observed test statistic falls within the critical region, *p-value* of the test statistic becomes less than α . In this case, H_0 is rejected. If the *p-value* of the test statistic is greater than α , the observed test statistic falls outside the critical region. In that case, H_0 will be accepted.

3. Goodness-of-fit Test

Goodness-of-fit test is a statistical procedure to decide whether sample data comes from a particular distribution or not. This is a specific hypothesis testing where H_0 : Sample data comes from a distribution to be tested. H_a : Sample data not from that distribution.

Chi-square (χ^2) test [76], Kolmogorov–Smirnov test (KS test) [77], and Anderson–Darling test [78] are some

examples of the goodness-of-fit test [79]. Out of these tests, the last two tests are designed for continuous distributions only. However, the KS test is modified later to consider discrete distributions as well [80]. The χ^2 test has been found more robust than the KS test for the continuous distributions [81].

C. Randomness Testing Suites

Randomness testing is very important to ensure whether an RNG is producing perfect random numbers or not. It tells us about the uniformity of the underlying distribution that the outputs of an RNG follow.

Definition 1. Let $S_k = \{0, 1\}^k$ be the set of all k -bit binary strings containing 2^k elements. A n -bit string, $X = x_1x_2 \dots x_n$, $x_i \in \{0, 1\}$ for all i , is called perfect (or uniformly) random if and only if for any k -bit ($k \leq n$) sub-string $x = x_jx_{j+1} \dots x_{j+k}$, for some $j \leq n - k$, of this string, the probability that $x = y$ for any $y \in S_k$ is $\frac{1}{2^k}$. That is,

$$X = x_1x_2 \dots x_n, x_i \in \{0, 1\} \forall i, \text{ is true random} \\ \iff \forall k < n, \forall j \leq n - k \text{ and } \forall y \in S_k, P(x = y) = \frac{1}{2^k},$$

where $x = x_jx_{j+1} \dots x_{j+k}$.

This definition of a perfect random number uses probability over all possible combinations of the bit string to ensure randomness. However, in a practical case, when we have only a finite sample, this probability cannot be perfectly calculated. Hence this definition cannot be directly used to test the randomness of random numbers.

To overcome this limitation, several randomness testing suites like NIST [11], Dieharder [12], AIS-31 [13], ENT [14] etc. have been proposed. Recently, Foreman et al. also suggested some test suite [82] for testing randomness. Each of these suites consists of multiple tests to decide the randomness of the input data. For each test, they calculate the value of the test statistic, and depending on these values the randomness is decided. NIST and Dieharder perform hypothesis testing with the null hypothesis that *the number is random*, AIS-31 performs interval estimation, and ENT directly returns the test statistic values. These suites consider different aspects, such as entropy, serial correlation, frequency of values, repetition of similar patterns etc. to perform the test. Some tests also perform Monte Carlo simulation [2] to validate the randomness.

III. REVISITING QRNG BASED ON SINGLE-PHOTON SOURCE

QRNG, based on single photons, uses 50/50 beam splitter [83], where an *R/T beam-splitter* denotes an optical device that splits an incoming light beam into $R\%$

reflected and $T\%$ transmitted light beams. A standard technique is to place a 50/50 Beam-splitter making an angle of 45° with the path of the photons. Thus, a single photon either passes through the beam-splitter, or it is reflected with probability $\frac{1}{2}$. Two photon detectors say D_0 and D_1 , can be placed over two output paths. If a photon is detected by D_i , i is registered as a random bit. A block diagram of this process is given in Fig. 1.

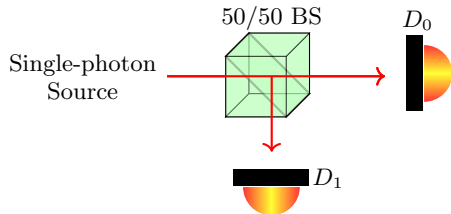


FIG. 1. A generic block diagram of the single-photon-based QRNG. Single-photon, coming from the source, are sent through a 50/50 beam-splitter. Two SPDs (D_0, D_1) are placed in two paths to detect the photon. Photon may take either path with probability 0.5. The random bit would be i if the detection happens at D_i .

If the photon source for this QRNG is not a perfect single-photon source, it may happen that at the same time some photons are transmitted through the beam-splitter and some are reflected. Then, both the detectors may detect photons simultaneously, and the random number cannot be generated. To ensure whether the source is a single-photon source or not, one may perform the first step of the two-fold statistical method mentioned in Section V. If this method reveals that the distribution is not sub-Poissonian, then the source cannot be a single-photon source, and that source cannot be used in this QRNG.

Each bit of the random number generated with this single-photon-based QRNG has probability $\frac{1}{2}$ of being 0 or 1. So, ideally it produces uniform random numbers. However, any defect in the beam-splitter or the detectors may change this probability. For example, consider an R/T beam-splitter and the detectors D_i with detection efficiency $d_i \in (0, 1]$. Suppose, D_0 is placed on the path of the transmitted light, and D_1 is placed on the path of the reflected light. Then the probability of 0 in the generated random number, that is, the probability of detecting a photon by detector D_0 would be

$$P(D_0) = \frac{d_0}{d_0 + d_1} \frac{T}{100}. \quad (5)$$

Similarly, the probability of 1 would be

$$P(D_1) = \frac{d_1}{d_0 + d_1} \frac{R}{100}. \quad (6)$$

If $d_0T \neq d_1R$, the generated random number would not be uniformly random. To test this randomness, statistical tests like NIST, Dieharder, AIS-31, ENT etc. may be used. See Section VIII for a discussion on these.

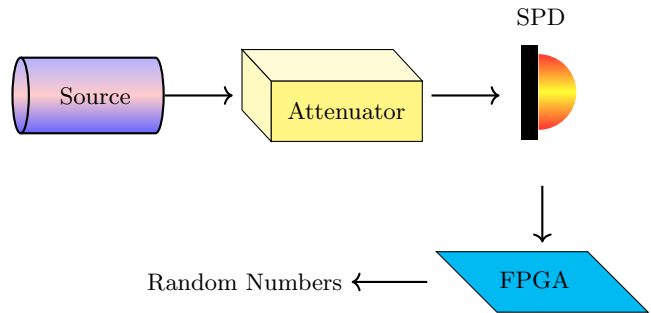


FIG. 2. A basic block diagram of the photon arrival time-based QRNG using weak coherent pulses. Coherent pulses, coming from the source, are sent through attenuators to reduce their power so that the probability of having multiple photons within a predefined time interval becomes negligible [84]. A SPD detects these photons and the detection time (photon arrival time) has been registered. The Field Programmable Gate Array (FPGA) provides random numbers based on the registered time stamps.

IV. REVISITING QRNG BASED ON COHERENT PULSE

It is well known that producing single photon states is experimentally challenging [57, 58]. However, different experimental approaches [59–66] have been performed to produce single photons. One of the approaches is using a coherent photon source followed by attenuators. This approach produces photon pulses with negligible probability of having multiple photons within a time interval [84]. In this process, the photons follow Poissonian statistics. A generic block diagram of the photon arrival time-based QRNG using photons from coherent sources is given in Fig. 2.

If λ is the wavelength of the photon wave and n photons are present within T time, the corresponding photon power would be

$$P = \frac{n\hbar c}{\lambda T} = \frac{\mu\hbar c}{\lambda}, \quad (7)$$

where \hbar is the Planck's constant and c is the speed of light in vacuum. Let P_a be the photon power coming out from the attenuators. Then, the expected number of photons per unit time is given by

$$\mu = \frac{P_a \lambda}{\hbar c}. \quad (8)$$

This attenuated pulse is detected by the SPD. The time of this detection is registered to produce photon arrival time-based random numbers.

There are different methods to produce random numbers from the registered times. Time diagrams for these methods are shown in Fig. 3. In Fig. 3(I), if the registered times of photon arrivals are $\{t_0, t_1, \dots, t_{2i-2}, t_{2i-1}, t_{2i}, \dots\}$, the non-overlapping consecutive time intervals, i.e., $\Delta t_{2i-1} = t_{2i-1} - t_{2i-2}$, $\Delta t_{2i} =$

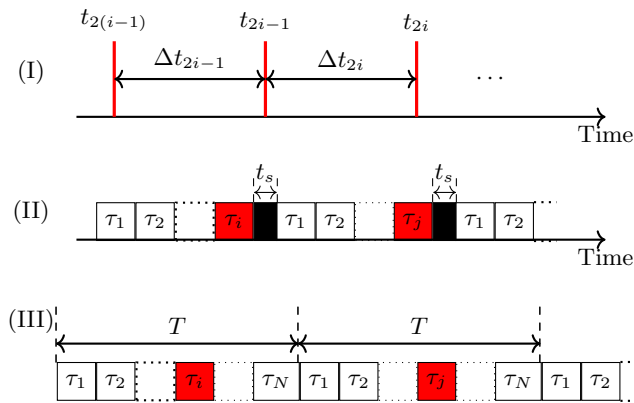


FIG. 3. Time diagram for the arrivals of the photons. There are three different methods to generate random numbers from photon arrival times. (I) Photons are detected in a continuous time reference at time $\{t_0, t_1, \dots, t_{2(i-1)}, t_{2i-1}, t_{2i}, \dots\}$. The i -th bit of the random number will be 0 if $\Delta t_{2i-1} < \Delta t_{2i}$ and 1 if $\Delta t_{2i-1} > \Delta t_{2i}$. (II) Time is divided into bins of equal length. If a photon has been detected in the i -th bin then $i - 1$ will be the corresponding random number. A new cycle of bins starts after a fixed sleep time (t_s) of the SPD. (III) An external time reference of cycle T has been used. Each cycle is divided into N equal time-bins $\tau_1, \tau_2, \dots, \tau_N$. For each cycle, if the first photon has been detected in i -th bin then $i - 1$ will be the corresponding random number. SPD will be in sleep mode for the remaining time of the cycle.

$t_{2i} - t_{2i-1}$, are used to generate random numbers as follows.

$$\begin{cases} \text{The } i\text{-th bit is taken as 0, if } \Delta t_{2i-1} < \Delta t_{2i}, \\ \text{The } i\text{-th bit is taken as 1, if } \Delta t_{2i-1} > \Delta t_{2i}. \end{cases} \quad (9)$$

But in this process [16], the random number generation rate is very slow. The length of the random bit-string is half of the photon count. Comparatively faster processes have been developed in the literature [15, 17–20]. In Fig. 3(II), the time is divided into time-bins, each having equal length. If a photon is detected in the i -th time-bin, $i - 1$ is taken as the random number. A new cycle of the bins starts after the detector has a fixed sleep time. Since the photon counting process is a Poisson process, the probability, that the waiting time (t_w) between the arrivals of two consecutive photons is greater than t , is given by

$$\begin{aligned} P(t_w > t) &= P(\text{no photon in } (0, t]) \\ &= P(0, t) = e^{-\mu t}. \end{aligned} \quad (10)$$

Therefore, the random number generated with this procedure follows exponential distribution [17–20]. Another QRNG scheme is proposed in [15], as depicted in Fig. 3(III), using external time reference. This external time is divided into cycles of length T , which is smaller than the dead time of the SPD. The time T is further divided into N equal subintervals, called the time-bins

$\tau_1, \tau_2, \dots, \tau_N$. In each cycle, if the first photon is detected in the i -th time-bin, $i - 1$ would be the corresponding random number. SPD would be in sleep mode for the remaining time of the cycle.

Let n photons be present within T time after the attenuation. Since the photon count follows Poisson distribution (4), the probability, that all the n photons are detected in the i -th interval, is given by

$$\begin{aligned} P(i; all | n) &= \frac{P(n, |\tau_i|)P(0, \frac{i-1}{N}T)P(0, T - \frac{i}{N}T)}{P(n, T)} \\ &= \frac{e^{-\mu|\tau_i|}(\mu|\tau_i|)^n e^{-\mu\frac{i-1}{N}T} e^{-\mu(1-\frac{i}{N})T}}{\frac{e^{-\mu T}(\mu T)^n}{n!}} \\ &= \frac{1}{N^n}. \end{aligned} \quad (11)$$

Here $|\tau_i|$ is the length of i -th time-bin, which equals $\frac{T}{N}$. Therefore, if only one photon is present within T time after the attenuation then that photon would be detected in the i -th bin with probability $\frac{1}{N}$. Thus the photon arrival time follows random distribution over the time-bins. However, this is the case, when exactly one photon is present in T time, and also when the detection is perfect. Since this is not a practical case, next we discuss the photon statistics for some practical scenarios.

V. OUR PROPOSAL OF TWO-FOLD STATISTICAL METHOD FOR TESTING QUANTUMNESS

In Section II A we have discussed that for the Poissonian distribution, the mean of the photon-counting distribution is the same as its variance. However, it is interesting to note that $mean = variance$ does not always imply that the distribution is Poisson. For example, consider the probability distribution

$$P(k) = (1 - p)^{k-1}p, k = 1, 2, 3, \dots, \quad (12)$$

for $0 \leq p \leq 1$. If $p = \frac{1}{2}$, this distribution also has mean = variance = 2. But, it is not Poisson.

Also, in experimental methods the means and variances are calculated from finite data samples. The fineness of the sample cannot perfectly reflect the mean and variances of the underlying distribution. Therefore, the comparison between the mean and the variance with equality may not reflect the underlying distribution undoubtedly.

This motivates us to propose a *two-fold method* to test the quantumness of the photon source as an answer to question Q1. First, a statistical test is performed to verify whether the mean is equal to or less than or greater than the variance. Note that any statistical validation of equality is not exact, but rather approximate in practice. Thus, if the above test validates the mean and the variance to be equal, we propose to perform a second test to validate that the distribution is indeed Poisson.

A. Interval Estimation

Since Poissonian and super-Poissonian statistics are explainable using classical theory, only sub-Poissonian distribution can guarantee the quantumness of a quantum device. We suggest a procedure to decide whether the underlying distribution is sup-Poissonian or not by estimating the confidence interval for the mean of the underlying distribution as follows.

Suppose, the number of photon counts within a fixed time is given as a sample of size n . Then by the central limit theorem, $\frac{\langle X \rangle - m}{\sigma/\sqrt{n}}$ is approximately standard normal for large n [75], where $\langle X \rangle$ is the random variable corresponding to the sample mean $\langle x \rangle$, and m, σ^2 are mean and variance of the actual photon-count distribution. Let the sample variance be given by S^2 . Then $s^2 = \frac{n}{n-1} S^2$ is an unbiased and consistent estimate of σ^2 [75]. Therefore, by replacing σ by s , we can say that $Y = \frac{\langle X \rangle - m}{s/\sqrt{n}}$ is approximately standard normal for large n .

Let $1 - \epsilon$ be the confidence level. Suppose y_ϵ be such that

$$P(-y_\epsilon < Y < y_\epsilon) \approx \frac{1}{\sqrt{2\pi}} \int_{-y_\epsilon}^{y_\epsilon} e^{-\frac{y^2}{2}} dy = 1 - \epsilon. \quad (13)$$

Then we have the probability

$$\begin{aligned} P(-y_\epsilon < Y < y_\epsilon) &= P(-y_\epsilon < \frac{\langle X \rangle - m}{s/\sqrt{n}} < y_\epsilon) \\ &= P(\langle X \rangle - \frac{sy_\epsilon}{\sqrt{n}} < m < \langle X \rangle + \frac{sy_\epsilon}{\sqrt{n}}). \end{aligned} \quad (14)$$

Therefore, combining Eq. (13) and Eq. (14), we have

$$P(\langle X \rangle - \frac{sy_\epsilon}{\sqrt{n}} < m < \langle X \rangle + \frac{sy_\epsilon}{\sqrt{n}}) = 1 - \epsilon. \quad (15)$$

So, we can say that $(\langle x \rangle - \frac{sy_\epsilon}{\sqrt{n}}, \langle x \rangle + \frac{sy_\epsilon}{\sqrt{n}})$ is an approximate confidence interval for the distribution mean m with confidence level $1 - \epsilon$.

Now we can decide the photon count distribution as sub-Poissonian, or super-Poissonian, with confidence level $1 - \epsilon$, if the estimated variance, $s \leq \langle x \rangle - \frac{sy_\epsilon}{\sqrt{n}}$, or $s \geq \langle x \rangle + \frac{sy_\epsilon}{\sqrt{n}}$, i.e., $\frac{\langle x \rangle}{s} \geq 1 + \frac{y_\epsilon}{\sqrt{n}}$, or $\frac{\langle x \rangle}{s} \leq 1 - \frac{y_\epsilon}{\sqrt{n}}$ respectively, where y_ϵ is given by Eq. (13). That is, for some given ϵ and y_ϵ given by Eq. (13),

$$\begin{aligned} \frac{\langle x \rangle}{s} \geq 1 + \frac{y_\epsilon}{\sqrt{n}} &\implies \text{sub-Poissonian distribution,} \\ \frac{\langle x \rangle}{s} \leq 1 - \frac{y_\epsilon}{\sqrt{n}} &\implies \text{super-Poissonian distribution,} \end{aligned} \quad (16)$$

with confidence level $1 - \epsilon$.

Alternatively, one can perform hypothesis testing to determine whether the light is sub-Poissonian, Poissonian, or super-Poissonian.

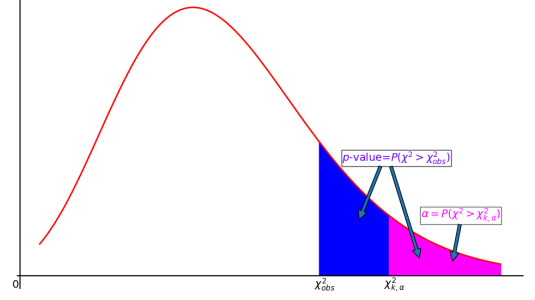


FIG. 4. Probability density function for χ^2 distribution. The critical region, $\chi^2 > \chi_{k,\alpha}^2$, for the χ^2 test is denoted by stars, and the region, $\chi^2 > \chi_{obs}^2$, corresponding to the p -value is denoted by dots. Since here $\chi_{k,\alpha}^2 > \chi_{obs}^2$, the p -value becomes larger than α and the region corresponding to the p -value contains the critical region. Therefore, in this case, the null hypothesis is accepted.

B. Hypothesis Testing

To determine the quantumness one has to perform two consecutive hypothesis testing. For the first test,

$$H_0 : m = s^2, H_a : m < s^2, \quad (17)$$

and for the second test,

$$H_0 : m = s^2, H_a : m > s^2. \quad (18)$$

For both tests, the test statistic would be $z = \frac{\langle x \rangle - s^2}{s/\sqrt{n}}$.

For the first test,

case 1: if $z \geq y_\epsilon$, where y_ϵ is given by Eq. (13), H_0 is rejected. That implies the underlying photon distribution is sub-Poissonian.

case 2: if $z < y_\epsilon$, we cannot reject H_0 . Also, we cannot accept H_0 due to lack of evidence. In that case, we have to perform second hypothesis testing with the same statistic. After the second test, if $z \geq y_\epsilon$, H_0 is rejected again, and we can say that the underlying distribution is super-Poissonian.

Note that, this hypothesis testing is equivalent to the above interval estimation technique, and both results in the same decision.

C. Goodness-of-fit Test

Since the equality of mean and variance may not imply Poisson distribution, to ensure the Poisson distribution which is an indicator of a coherent source of light, we suggest a second test which is a goodness-of-fit test, that is, a hypothesis testing to decide whether a sample data comes from a Poisson distribution or not.

For testing the quantumness in the generated random number, one may use the χ^2 goodness-of-fit test [75, 85]

on the data generated by QRNGs as follows. Consider null and alternative hypotheses as

H_0 : The data follow the distribution (4).

H_a : The data do not follow the distribution (4).

The test statistic is defined as

$$\chi^2 = \sum_{n=1}^N \frac{(O_n - E_n)^2}{E_n}, \quad (19)$$

where O_n denotes the frequency of n number of photon in the data, E_n denotes the frequency given by Poisson distribution (4). This test statistic follows χ^2 distribution with $k = N - 1$ degrees of freedom if all the parameters are known, and its density function is given by,

$$f_{\chi^2}(x) = \frac{x^{\frac{k}{2}-1} e^{-\frac{x}{2}}}{2^{\frac{k}{2}} \Gamma(\frac{k}{2})}, \quad x \geq 0, \quad (20)$$

$$\text{where } \Gamma(z) = \int_0^{\infty} t^{z-1} e^{-t} dt$$

is the well-known Gamma function [75]. The cumulative distribution function in this case is given by,

$$F_{\chi^2}(z) = \int_0^z f_{\chi^2}(x) dx. \quad (21)$$

Figure 4 is a plot of the probability density function of a χ^2 distribution. The critical region ($\chi^2 > \chi_{k,\alpha}^2$) for the χ^2 test is denoted by stars, and the region corresponding to the p -value ($\chi^2 > \chi_{obs}^2$) is denoted by dots. The area of the critical region is given by

$$P(\chi^2 > \chi_{k,\alpha}^2) = 1 - F_{\chi^2}(\chi_{k,\alpha}^2) = \alpha. \quad (22)$$

χ^2 -test being a one-tailed test, p -value for this test is given by

$$P(\chi^2 > \chi_{obs}^2) = 1 - F_{\chi^2}(\chi_{obs}^2), \quad (23)$$

where χ_{obs}^2 is the observed value of the test statistic.

If the typical values of the parameters μ, T in Eq. (4) are known, we have $k = N - 1$. However, if they are unknown, in that case, $k = N - 2$. Therefore, H_0 is rejected if $\chi_{obs}^2 > \chi_{k,\alpha}^2$, where $\chi_{k,\alpha}^2$ is the value given by $F_{\chi^2}(\chi_{k,\alpha}^2) = 1 - \alpha$. In other words, H_0 is rejected if p -value is less than α .

As in most cases, the equality of the mean and the variance denotes Poisson distribution, for practical purposes, the last χ^2 test may not be needed. We mention this test for the completeness of the discussion.

VI. DETAILED PHOTON COUNTING STATISTICS OF COHERENT PULSE-BASED QRNG

The statistics discussed in Eq. (11) of Section IV consider that all of the n photons present within time T would be detected in the same time-bin, which is a crude assumption for $n > 1$. In this section, we perform a more fine-grained analysis of the first photon arrival time for coherent pulse-based QRNG devices. This analysis helps us to investigate the quality of QRNG in terms of several parameters, as elaborated in Section VII.

A. Time-bin Statistics for Poissonian Photon with Perfect Devices

Currently available photon arrival time-based QRNGs [41, 42] use coherent sources, which generate photons that follow Poissonian statistics. Here, a random number is generated based on the detection time of the first photon in each time cycle T . The probability of detecting the first photon in i -th bin, when n photons are present within T time, is given by

$$\begin{aligned} P(i; 1st|n) &= \frac{\sum_{l=1}^n P(0, \frac{(i-1)T}{N}) P(l, \frac{T}{N}) P(n-l, T - \frac{iT}{N})}{P(n, T)} \\ &= \frac{\sum_{l=1}^n e^{-\mu T \frac{i-1}{N}} \frac{e^{-\mu T/N} (\frac{\mu T}{N})^l}{l!} e^{-\mu T(1-\frac{i}{N})} (\mu T)^{n-l} (1-\frac{i}{N})^{n-l}}{\frac{e^{-\mu T} (\mu T)^n}{n!}} \\ &= \sum_{l=1}^n \binom{n}{l} \left(\frac{1}{N}\right)^l \left(1-\frac{i}{N}\right)^{n-l} \\ &= \left(1-\frac{i-1}{N}\right)^n - \left(1-\frac{i}{N}\right)^n. \end{aligned} \quad (24)$$

However, we do not know the number of photons present

within the period T . Therefore, the probability of detecting the first photon in the i -th bin is given by

$$\begin{aligned}
P(i; 1st) &= \sum_{n \geq 0} P(i; 1st|n)P(n, T) \\
&= P(i; 1st|0)P(0, T) + \sum_{n > 0} P(i; 1st|n)P(n, T) \\
&= 0 + \sum_{n > 0} \frac{e^{-\mu T} (\mu T)^n}{n!} \left[\left(1 - \frac{i-1}{N}\right)^n - \left(1 - \frac{i}{N}\right)^n \right] \\
&= e^{-\mu T} \sum_{n > 0} \frac{[\mu T (1 - \frac{i-1}{N})]^n}{n!} - e^{-\mu T} \sum_{n > 0} \frac{[\mu T (1 - \frac{i}{N})]^n}{n!} \\
&= e^{-(i-1)\frac{\mu T}{N}} - e^{-i\frac{\mu T}{N}}.
\end{aligned} \tag{25}$$

B. Time-bin Statistics for Poissonian Photon with Imperfect Devices

Till now, we have considered all of the used optical devices as ideal. But in practice, any error in the source and in the attenuators affects photon power and changes the value of the mean photon number per unit time. Again, if the detector is not 100% efficient, The first photon would

be detected in the i -th time-bin, if at least one photon has been detected in i -th bin, and either (A) no photon has been reached at SPD before the i -th bin, or (B) k number of photons have reached before the i -th bin, but none of them has been detected. Therefore, the probability of detecting the first photon in the i -th bin, when n photons are present within T time, is given by

$$\begin{aligned}
P_d(i; 1st|n) &= \frac{\sum_{k=0}^{n-1} P(k, \frac{(i-1)T}{N})(1-d)^k \sum_{l=1}^{n-k} \{1 - (1-d)^l\} P(l, \frac{T}{N}) P(n-k-l, T - \frac{iT}{N})}{P(n, T)} \\
&= \frac{\sum_{k=0}^{n-1} \frac{e^{-\mu T \frac{i-1}{N}} (\mu T \frac{i-1}{N})^k}{k!} (1-d)^k \sum_{l=1}^{n-k} \{1 - (1-d)^l\} \frac{e^{-\mu T/N} (\frac{\mu T}{N})^l}{l!} \frac{e^{-\mu T(1-\frac{i}{N})} (\mu T)^{n-k-l} (1-\frac{i}{N})^{n-k-l}}{(n-k-l)!}}{e^{-\mu T} (\mu T)^n / n!}} \\
&= n! \sum_{k=0}^{n-1} \frac{\left(\frac{(i-1)(1-d)}{N}\right)^k}{k!} \frac{1}{(n-k)!} \sum_{l=1}^{n-k} \binom{n-k}{l} \left[\left(\frac{1}{N}\right)^l \left(1 - \frac{i}{N}\right)^{n-k-l} - \left(\frac{1-d}{N}\right)^l \left(1 - \frac{i}{N}\right)^{n-k-l} \right] \\
&= \sum_{k=0}^{n-1} \binom{n}{k} \left(\frac{(i-1)(1-d)}{N}\right)^k \left[\left(1 - \frac{i-1}{N}\right)^{n-k} - \left(1 - \frac{i-1+d}{N}\right)^{n-k} \right] \\
&= \left(1 - (i-1)\frac{d}{N}\right)^n - \left(1 - i\frac{d}{N}\right)^n,
\end{aligned} \tag{26}$$

where $d \in (0, 1]$ is the detection efficiency. Since the exact number of photons is unknown, the probability of detecting the first photon in the i -th bin becomes

$$\begin{aligned}
P_d(i; 1st) &= e^{-(i-1)\frac{\mu T d}{N}} - e^{-i\frac{\mu T d}{N}} \\
&= (e^{\frac{\mu T d}{N}} - 1)e^{-i\frac{\mu T d}{N}}.
\end{aligned} \tag{27}$$

The remaining probability

$$1 - \sum_{i=1}^N P_d(i; 1st) = e^{-\mu T d} \tag{28}$$

is the probability of detecting no photon in a complete reference cycle. In that case, this reference cycle has no contribution to the random number. Therefore the probability mass function of the distribution corresponding to

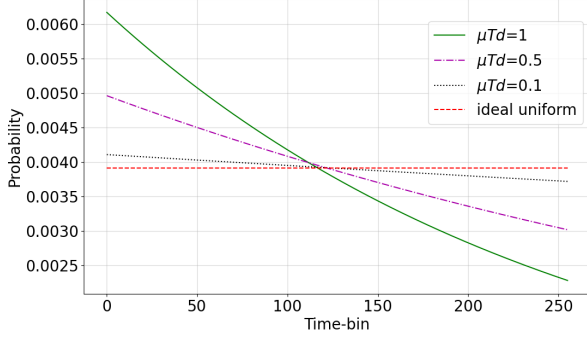


FIG. 5. Plots for the probabilities of detecting the first photon in 256 time-bins. Probabilities for different values of μTd as well as uniform probability distribution have been plotted. μ is the expected number of photons in unit time, T is the time cycle in the external reference time frame, and d is the detection efficiency. If all the optical components are ideal then the distribution should be given by red dashed line.

the detection of the first photon in the i -th bin is given by

$$f(i) = \frac{e^{\frac{\mu Td}{N}} - 1}{1 - e^{-\mu Td}} e^{-i\frac{\mu Td}{N}}, \quad i = 1, 2, \dots, N. \quad (29)$$

Figure 5 shows how μTd affects the probability (29). Here we consider $N = 256$. From this plot, it is clear that the randomness increases as μTd decreases. Therefore, the main goal in designing a QRNG is

$$\begin{aligned} & \underset{\mu, T, d}{\text{minimize}} \quad g(\mu, T, d) := \mu Td, \\ & \text{subject to } \mu > 0, T > 0, d > 0. \end{aligned} \quad (30)$$

However, this minimization is bounded by some constraints related to the generation rate, the cost and the timing error in registering the photon detection time. These constraints are discussed in Section VII.

Next, let us consider QRNG in Fig. 3(II). Here, the probability, that the waiting time (t_w) between the arrival of two consecutive photons lies in the i -th bin, is given by

$$\begin{aligned} P((i-1)t_l < t_w < it_l) &= P(t_w > (i-1)t_l) - P(t_w > it_l) \\ &= e^{-(i-1)\mu t_l} - e^{-i\mu t_l}, \end{aligned} \quad (31)$$

where t_l is the length of each time-bin. If the detection efficiency is given by d , this probability is given by

$$P_d((i-1)t_l < t_w < it_l) = e^{-(i-1)\mu t_l d} - e^{-i\mu t_l d}. \quad (32)$$

Since in the probability distribution of Eq. (27), $\frac{T}{N}$ is the length of the time-bins, Eq. (32) is identical with Eq. (27). Therefore, the probability mass function corresponding to the probability Eq. (32) is also given by Eq. (29) with $T = Nt_l$.

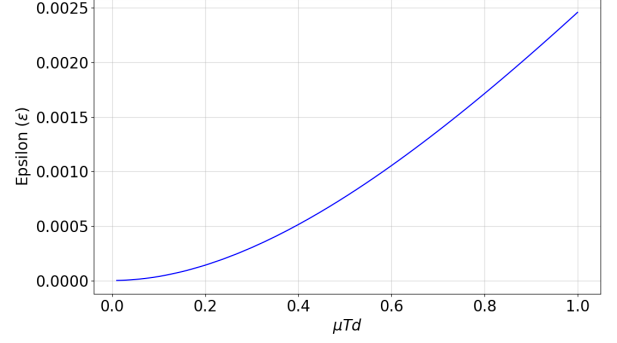


FIG. 6. Plot representing the relation between μTd and ϵ such that the probability distribution given by Eq. (29) is ϵ -random. Randomness reduces as μTd increases. This product can be reduced with the proper choice of external reference cycle T , and proper tuning of the source, the attenuators and the detector.

Therefore, these two types of QRNGs, perform similarly in practical scenarios. However, if we can ensure that the source is an actual single-photon source, then the perfect random number can be generated using an external time reference with probability distribution $P_d(i) = \frac{d}{N}$ (Ref. Eq. (11)). Since the distributions given by Eq. (29) are evaluated from the quantum properties of photons, this can be used to test the quantumness in a QRNG.

Definition 2. We define a probability distribution $P(\cdot)$, with support S , as ϵ -random if and only if

$$\max_{i, j \in S} |P(i) - P(j)| = \epsilon. \quad (33)$$

Since the distribution (29) is a monotone decreasing function, it becomes ϵ -random if and only if

$$\begin{aligned} f(1) - f(N) &= \epsilon \\ \implies \frac{e^{\frac{\mu Td}{N}} - 1}{e^{\mu Td} - 1} \left(e^{(1-\frac{1}{N})\mu Td} - 1 \right) &= \epsilon. \end{aligned} \quad (34)$$

Figure 6 is a visual representation of the Eq. (34). It clearly shows that the value of ϵ increases with μTd . That means, to generate numbers with ϵ -randomness, we need to carefully choose the external reference cycle T , and configure the source, the attenuators and the detector so that relation (34) has been satisfied.

We have performed the NIST, Dieharder, AIS-31 and ENT tests on the data generated by simulating the probability distribution given by Eq. (29). These test results are provided in Section VIII.

VII. EFFECT OF μ, T, d ON RANDOM NUMBER GENERATION RATE AND COST

As discussed in Eq. (30) of Subsection VIB, we have to minimize μTd to achieve maximum randomness from

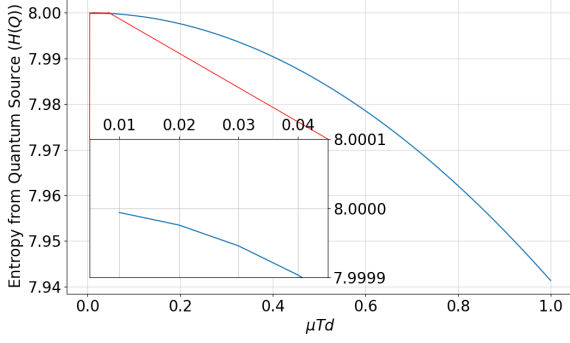


FIG. 7. Entropy (38) of the probability distribution (29). When the product of the expected number of photons, μT , within an external reference cycle T , and the detection efficiency d is very small, the entropy $H(Q)$ of the distribution generated by the QRNG is very close to the entropy $H(U) = 8$ of the uniform random distribution. Therefore, if $\mu T d$ is very small, the random number generated by the QRNG would be close to the uniform random number.

the quantum source increases. In that discussion, we have considered the product $\mu T d$ as a single quantity. In this section, we separately discuss the effect of

- the expected photon number in unit time, μ ,
- the external reference cycle, T , and

$$H(Q) = \frac{1 - (N + 1)e^{-\mu T d} + N e^{-(N+1)\frac{\mu T d}{N}}}{(1 - e^{-\mu T d})(1 - e^{-\frac{\mu T d}{N}})} \log \left(e^{\frac{\mu T d}{N}} \right) - \log \left(\frac{e^{\frac{\mu T d}{N}} - 1}{1 - e^{-\mu T d}} \right). \quad (38)$$

A detailed derivation of this entropy has been added in Appendix B. Fig. 7 shows how the entropy (38) changes with $\mu T d$. Here we have chosen $N = 256$. Therefore, the entropy (37) of the uniform distribution would be $H(U) = \log 256 = 8$. From Fig. 7, it can be easily seen that, if $\mu T d$ is very small, the entropy $H(Q)$ is very close to 8, which is the entropy of the uniform distribution. In this section, by *randomness* we will refer to the randomness due to $H(Q)$ only.

A. Effect of the Expected Photon Numbers

Here we discuss the effect of the expected photon numbers on the cost as well as the random number generation rate of a QRNG.

- the detection efficiency, d

on the rate of random number generation, r as well as on the cost of the QRNG.

The *entropy*, which is the source of randomness of a QRNG, can be expressed as

$$H(E) = H(Q) + H(C), \quad (35)$$

where, $H(E)$, $H(Q)$ and $H(C)$ are the total entropy generated by the RNG, the entropy of the quantum source and the entropy of the classical source respectively.

Definition 3. An RNG is said to be perfect if $H(E) = H(U)$, where $H(U)$ is the entropy of uniform randomness. A QRNG is said to be perfect if $H(U) = H(E) = H(Q)$.

However, in the practical scenario, perfect QRNG is not possible. Therefore, the main goal in designing a QRNG is

$$\text{Goal: } H(Q) \approx H(U). \quad (36)$$

The Shannon entropy [86, 87] of a uniform distribution over N points is given by

$$H(U) = - \sum_{i=1}^N \frac{1}{N} \log \frac{1}{N} = \log N. \quad (37)$$

On the other hand, the entropy of the probability distribution (29) is given by

1. Effect of the Exected Photon Number on Cost

Since μ is the expected number of photons in unit time, this can be reduced by using heavy attenuation. This will directly affect the cost. Heavy attenuation requires a large number of high-quality attenuators, increasing the production cost for the random numbers. Thus

$$\text{small value of } \mu \implies \text{high production cost.} \quad (39)$$

2. Effect of the Expected Photon Number on Random Number Generation Rate

A small value of μ , which indicates a small number of photons, leads to a high chance of *no photon detection* in a particular external reference cycle of time interval T . That means those intervals will have no contribution

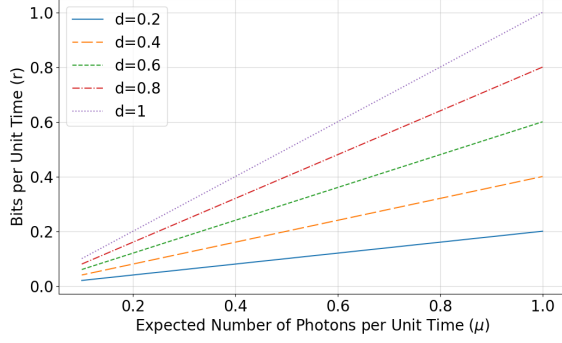


FIG. 8. Plot shows how random number generation rate (bit per unit time) changes with the expected photon number per unit time (μ). Five different plots have been shown for five different values of detection efficiency (d). From the plot, it can be easily seen that if μ decreases, the random number generation rate of the QRNG will also decrease.

to the final random number. Therefore, we require more cycles to produce random numbers of expected length. This will reduce the speed of the RNG. From Eq. (27), the probability, $P(0)$, of no photon detection within time T is given by

$$P(0) = 1 - \sum_{i=1}^N P_d(i; 1st) = e^{-\mu T d}, \quad (40)$$

where $P_d(i; 1st)$ is the probability of detecting the first photon in the i -th bin.

Suppose, for some μ , the expected number of external cycles to produce a random number of length k , where each cycle contains N time-bins, is given by N_c . Then $N_c = \langle X \rangle$, where X is a random variable, whose probability distribution is negative binomial distribution, given by

$$P(X = x) = \binom{x-1}{k'-1} (1 - P_\mu(0))^{k'} P_\mu(0)^{x-k'}, \quad (41)$$

for $x = k', k'+1, k'+2, \dots$, where $k' = \lceil \frac{k}{\log_2 N} \rceil$ and $P_\mu(0) = e^{-\mu T d}$. Therefore,

$$N_c = \langle X \rangle = \frac{k' P(0)}{1 - P(0)} = \frac{k'}{e^{\mu T d} - 1}. \quad (42)$$

Thus, the rate of generating random numbers is given by

$$r = \frac{k'}{T N_c} = \frac{e^{\mu T d} - 1}{T} \text{ bits per unit time.} \quad (43)$$

Since the external time cycle T is very small, Eq. (43) can be written as

$$r \approx \mu d \text{ bits per unit time.} \quad (44)$$

Clearly, if μ decreases, this rate will also decrease. The graph in Fig. 8 shows how this rate changes with μ for fixed T and d . Therefore, we cannot reduce μ arbitrarily to get the maximum amount of randomness.

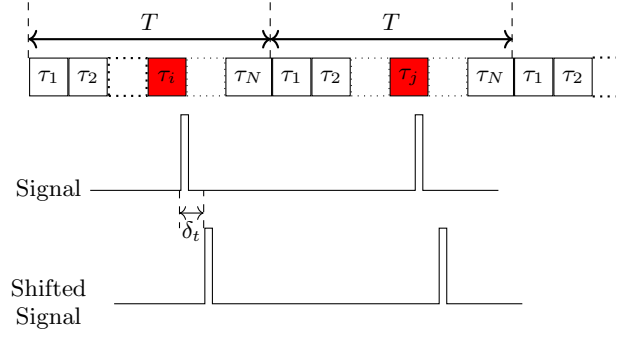


FIG. 9. Due to the timing error δ_t , the actual may be read as the shifted signal and the registered time-bin may be different from the actual time-bin of photon detection. This would add an error in the generated random number. To minimize such error, we put a lower bound on the external reference cycle T using Eq. (46).

B. Effect of the timing error of the device on the External Reference Cycle

If we choose the external reference cycle T very small, the product $\mu T d$ would also be small. This should increase the randomness, as discussed in Eq. (30) of the Subsection VI B. However, a small T would lead to a small length $\frac{T}{N}$ for the time bins. Now, if there are maximum δ_t errors in registering the photon-arrival-time, due to small time-bins, the time may be registered in a time-bin that is different from the actual time-bin as shown in Fig. 9. Let us consider that the actual detection happens in i -th bin, that is, within time interval $[(i-1)\frac{T}{N}, i\frac{T}{N}]$. If the actual detection happens within time interval $[(i-1)\frac{T}{N}, (i-1)\frac{T}{N} + \delta_t]$, the time may be registered as $(i-1)$ -th bin. Similarly, if the actual detection happens within time interval $[i\frac{T}{N} - \delta_t, i\frac{T}{N}]$, the time may be registered as $(i+1)$ -th bin. However, if the actual detection lies within the time interval $[(i-1)\frac{T}{N} + \delta_t, i\frac{T}{N} - \delta_t]$, there will be no error.

Now let us consider that T is chosen to satisfy the relation

$$\frac{T}{N} \geq k \delta_t, \quad (45)$$

for some suitable k . Then the probability, p_e , that the detection happens in i -th bin but outside of the interval $[(i-1)\frac{T}{N} + \delta_t, i\frac{T}{N} - \delta_t]$ is bounded above as $p_e \leq \frac{2}{k}$. Here we have assumed uniform distribution as the time $\frac{T}{Nk}$ is very small. Therefore, for a fixed error tolerance, p_{tol} , k can be chosen as $k_{tol} = \frac{2}{p_{tol}}$. In that case, the minimum reference cycle T_{min} should be

$$T_{min} = N k_{tol} \delta_t. \quad (46)$$

Therefore, we cannot make T arbitrarily small to get the maximum amount of randomness.

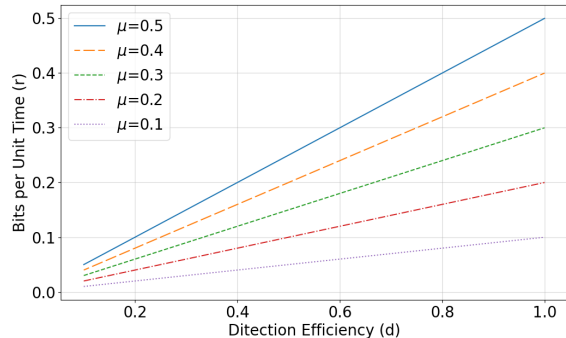


FIG. 10. Plot shows how random number generation rate (bit per unit time) changes with the detection efficiency (d). Five different plots have been shown for five different values of μ , the expected photon number per unit time. From the plot, it can be easily seen that if d decreases, the random number generation rate of the QRNG will also decrease.

C. Effect of the Reference Cycle on Random Number Generation Rate and Cost

Equation (44) indicates that T does not have much effect on the rate of generating random numbers. Also, since T has no impact on the used optical devices, it does not affect cost.

D. Effect of Detection Efficiency

In this subsection, we discuss the effect of the detection efficiency of the detector used in the QRNG on the cost as well as the random number generation rate of a QRNG.

1. Effect of the Detection Efficiency on Cost

The value of $\mu T d$ can be decreased by choosing a detector with bad detection efficiency. It is very natural that if a detector can efficiently detect photons, its cost will also be high. Since the randomness increases if $\mu T d$ decreases, choosing small d we can increase the randomness. This will also reduce the cost of the QRNG. Thus

$$\text{small value of } d \implies \begin{cases} \text{high randomness} \\ \text{high cost} \end{cases} \quad (47)$$

2. Effect of the Detection Efficiency on Random Number Generation Rate

Although a bad detector with a small detection efficiency, d , reduces production costs, this leads to a high chance of *no photon detection* in a particular external reference cycle. From Eq. (44) it can be easily seen that if T decreases, the rate of generating random numbers

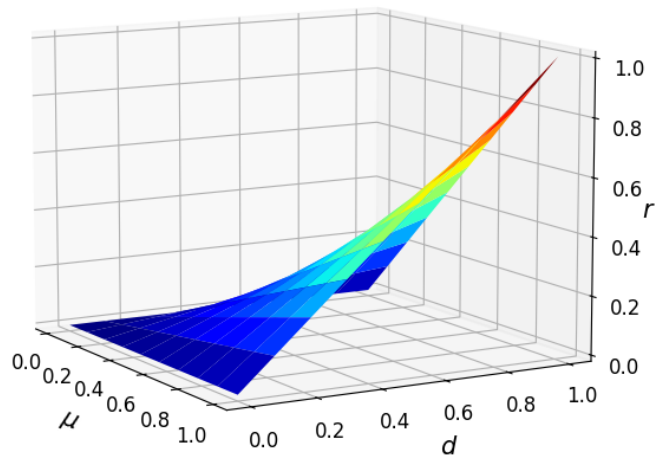


FIG. 11. Plot showing relation between random number generation rate, r , expected photon number in unit time, μ , and detection efficiency, d . If the values of μ and d are small, the generation rate is also small. Therefore, to generate random numbers with high rate, we have to choose both μ and d large.

Parameters ↓	Effects on		
	Randomness	Rate	Cost
μ	↑	↓	↑
T	↑	—	—
d	↑	↓	↓

TABLE I. The effects of decreasing the expected photon count μ , the external reference cycle T and the detection efficiency d . A down-arrow, ↓, denotes the decrement of the corresponding quantity. On the other hand, an up-arrow, ↑, denotes the increment. T does not affect speed or cost. If the parameters increase, the effects will be in the reverse direction.

will also decrease. The graph in Fig. 10 shows how this rate changes with μ for fixed T and d . Therefore, it is not possible to choose a detector with arbitrarily small detection efficiency.

E. Performance and Cost of the QRNG

Figure 11 is a surface plot of how the random number generation rate of the QRNG changes with μ and d . This shows that we have to consider high values of μ and d to get a high rate. On the other hand, in Eq. (30) of Subsection VIB we show that to get maximum randomness from the quantum source, we have to minimize the product $\mu T d$ small. Therefore, this needs some optimization while choosing μ and d .

The above discussion has been described as a heat map in Fig. 12. In the figure, dark shade denotes low value and light shade denotes high value of randomness, generation rate and cost in Figures 12(a), 12(b) and 12(c) respectively. Figure 12(a) shows that high randomness demands a small value of the product $\mu T d$. However, the product μd cannot be very small as Fig. 12(b) indi-

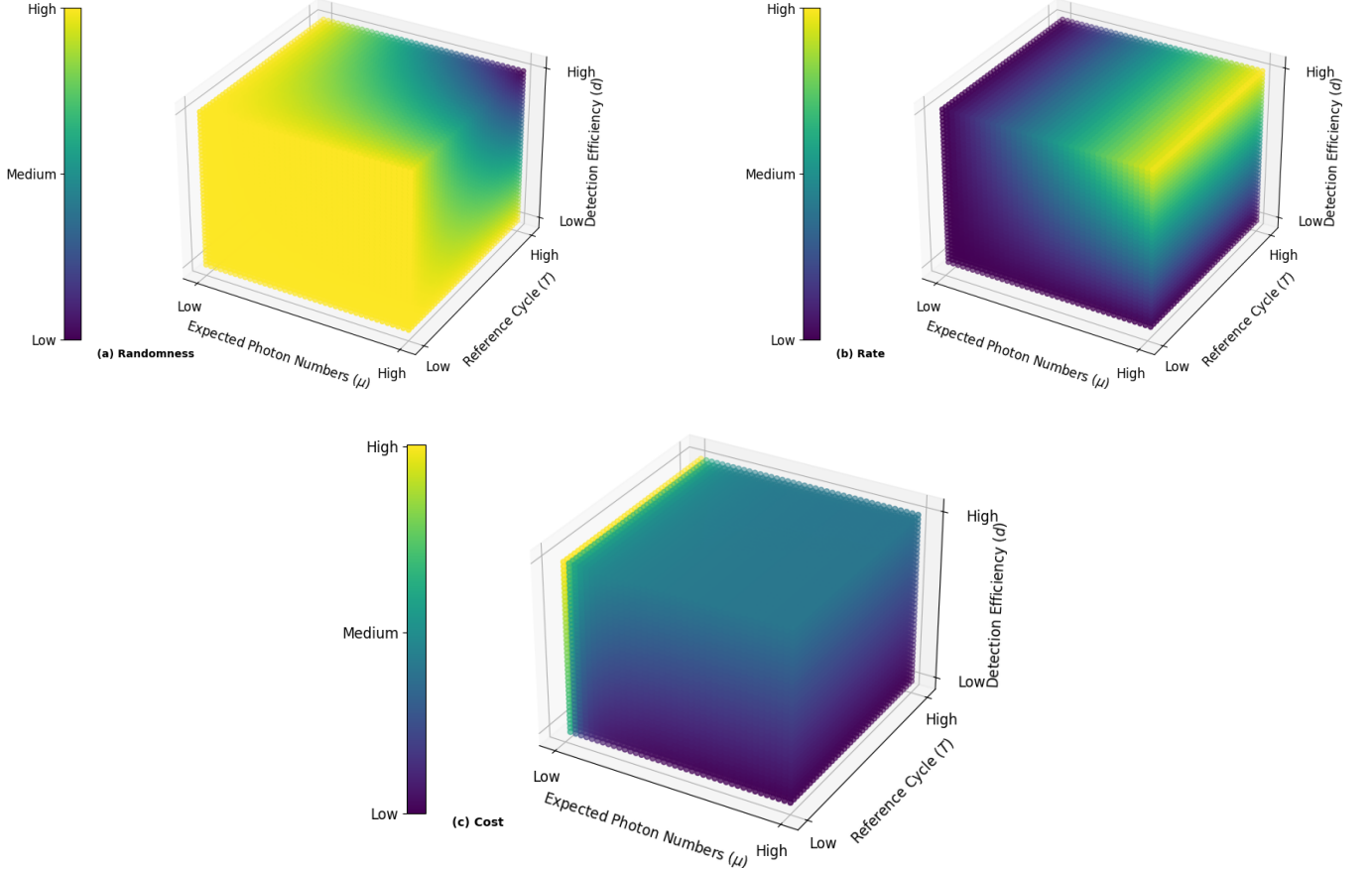


FIG. 12. Heat map denoting how (a) randomness, (b) random number generation rate and (c) cost varies depending on the expected photon number per unit time, μ , external reference cycle, T and the detection efficiency, d . Figure (a) shows that we must keep the product $\mu T d$ small to get maximum randomness. However, (b) shows if the μd is small, the generation rate will be minimal. On the other hand, from (c), low-cost demands a small value of d and a high value of μ .

cates. A small μd would result in a low random number generation rate. On the other hand, to keep the cost of the QRNG low, we need a small d but a large μ .

In Table I, we summarize the discussion in tabular form. A down-arrow (\downarrow) indicates a decrease in the value of the corresponding quantity, while an up-arrow (\uparrow) signifies an increase. The external reference cycle T does not influence speed or cost. If the parameters are increased, the effects will reverse accordingly.

We have already mentioned in Eq. (36) that the main goal in designing a QRNG is to keep $H(Q)$, the entropy from the quantum source as close as $H(U)$, the entropy of uniform randomness. However, we also discussed that this is not the only goal. There are some other constraints as well like random number generation rate and cost. A QRNG should generate random numbers with high rates and low costs. The randomness and the rate together describe the *performance* of the QRNG. Therefore, the goal in designing a QRNG is to maximize the performance and minimize the cost by choosing appropriate μ , T and d .

VIII. RESULTS OF RANDOMNESS TESTS

As mentioned in Subsection II C, the randomness of the random numbers is tested using statistical tests. Here we used four common statistical testing suites namely NIST, Dieharder, AIS-31 and ENT.

The NIST Randomness Testing Suite is an extensive set of statistical tests developed by the National Institute of Standards and Technology (NIST) to evaluate the quality of randomness in random numbers. It is one of the most widely used suites for testing randomness. It contains 15 different tests to examine different aspects of randomness. Most of the tests have the standard normal or χ^2 as reference distribution for their test statistic. Here null hypothesis is taken as *the number to be tested is random*. For each test, the significance level is considered as 0.01. If the value of the test statistic for some tests falls in the critical region, or equivalently, calculated p -value is less than 0.01, then the corresponding tests fail rejecting the null hypothesis. A perfectly random number should pass all of the 15 tests. As mentioned in Section V, the

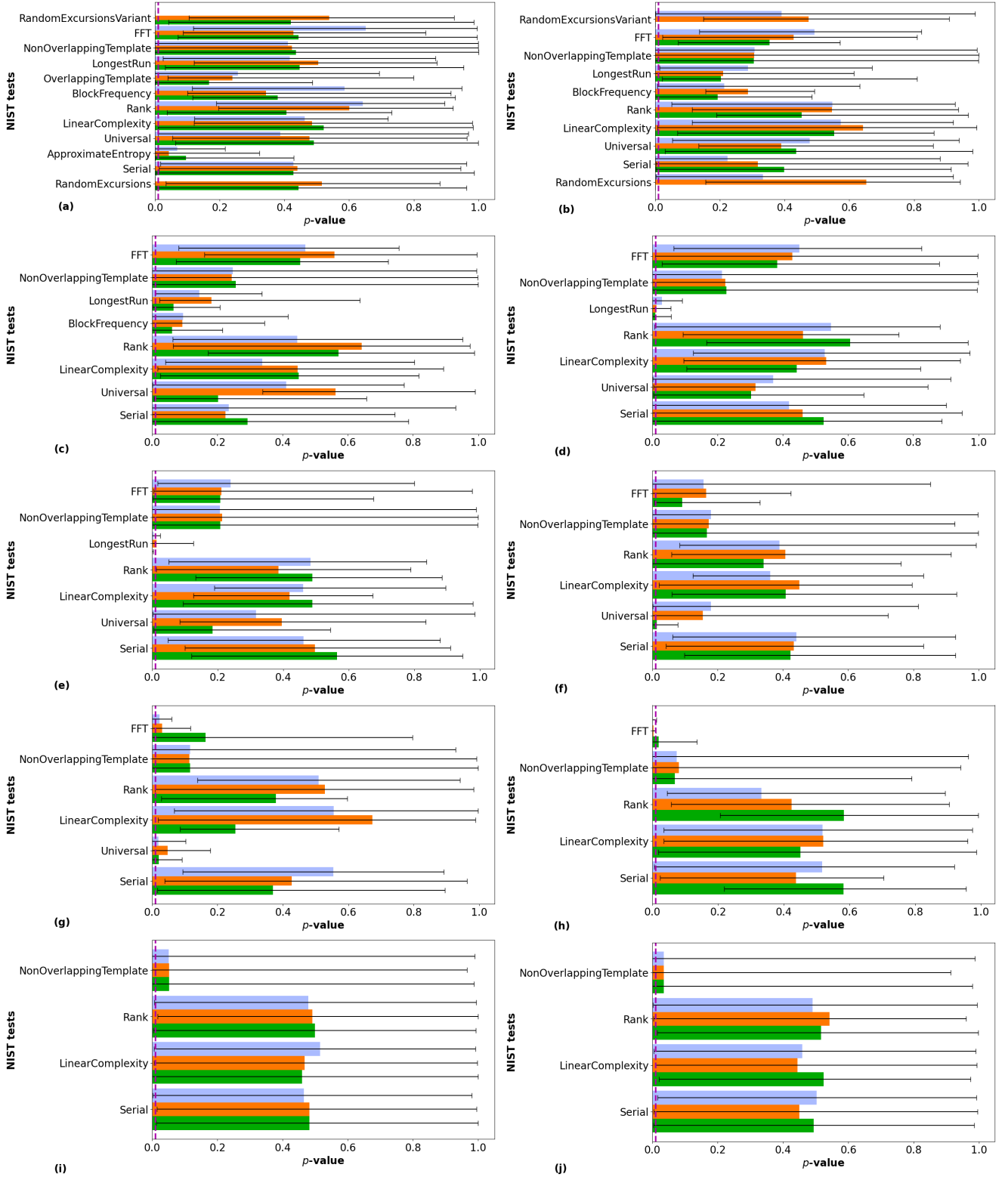


FIG. 13. NIST result. Bar charts are plotted for (a) $\mu Td = 0.05$, (b) $\mu Td = 0.10$, (c) $\mu Td = 0.15$, (d) $\mu Td = 0.20$, (e) $\mu Td = 0.25$, (f) $\mu Td = 0.30$, (g) $\mu Td = 0.35$, (h) $\mu Td = 0.40$, (i) $\mu Td = 0.45$, (j) $\mu Td = 0.50$. For each μTd , three 1 GB files are generated by simulating probability distribution (29), and the NIST tests have been performed on those files. Different textures denote results corresponding to different files. A test is considered as passed if the corresponding p -value is at least 0.01. Tests that fail for all of the three files are not included in the bar chart. The vertical dashed line denotes p -value = 0.01

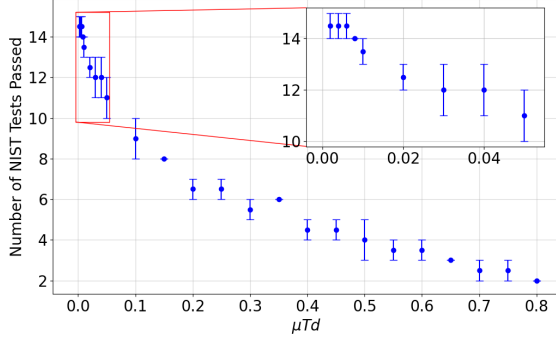


FIG. 14. NIST test results for the data simulated with the distribution given by Eq. (29). Three files, each containing 1 GB random number have been used for the test for every μTd . A test fails if the corresponding p -value is found less than 0.01. The range in the second column arises due to different results from three different files. The number of passed tests decreases with the increment of μTd . This indicates that as μTd increases, the randomness in the generated random number decreases.

central limit theorem is applicable only for large n , tests that use the central limit theorem to determine the reference distribution, have a requirement for the bit stream, that is, the length of the testing sequence, to be large enough (at least 10^6).

The *Dieharder* tests represent a battery of statistical tests used to assess the quality and randomness of a RNG. This suite contains around 30 tests for the assessment. These tests consider KS test of uniformity to obtain the p -values. Depending on these p -values, the decision (*passed*, *weak* or *failed*) has been taken. The results that do not pass and also do not have enough evidence to declare as fail have been mentioned as weak.

AIS-31 is a standardized suite of statistical tests for assessing RNGs. This suite comprises a total of 9 tests, typically organized into two main groups. Procedure A, consists of 6 tests aimed at detecting statistically inconspicuous behavior in RNG output. Procedure B, focuses on evaluating the internal random bits of TRNGs through 3 specific tests. These tests ensure that RNGs meet rigorous statistical criteria for randomness, providing a reliable measure of their quality and suitability for applications requiring secure and unpredictable random numbers.

ENT performs 5 tests on the stream of bytes and produces the outputs for each test. It calculates entropy, χ^2 statistic value, the arithmetic mean of the bytes, the Monte Carlo value of π and the serial correlation coefficient. Depending on these values user can decide the randomness.

We have generated random numbers simulating the probability distribution given by Eq. (29) for different μTd . Three files of size 1 GB have been generated for every μTd . Then we perform the NIST tests over the generated numbers. 100 bit streams of length 10, 000, 000

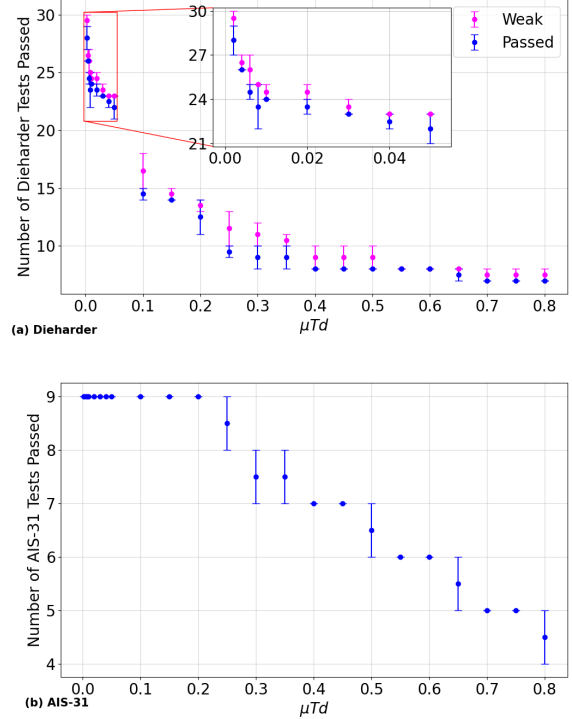


FIG. 15. (a) Dieharder and (b) AIS-31 test results for the data simulated with the distribution given by Eq. (29). For Dieharder, there are 30 tests; for AIS-31, 9 tests are there. These tests also reveal that the number of passed tests decreases as μTd increases indicating lower values of μTd result in better randomness before post-processing. Along with pass and fail, Dieharder tests also mention suspected results as weak. They are also included in this figure.

have been considered for the tests. In Fig. 13, we plot the bar charts of the p -values from different NIST tests. The tests for which the p -values are found as 0 are not included in the plot. From these plots, we can see that, as μTd increases, the number of passed tests decreases indicating a decrement of the randomness in the random number. The overall result is plotted in Fig. 14 as the number of tests our simulated data passed. These graphs indicate that lower μTd values give rise to better random numbers requiring less post-processing.

We have also performed the Dieharder, AIS-31 and ENT over the generated numbers. Figure 15 shows how many tests for our simulated data passed for Dieharder and AIS tests. Similar to the NIST tests, these tests also show that small μTd values provide better randomness before post-processing. ENT test does not mention pass or fail as a result. However, it provides ideal and actual values for the performed tests. In Fig. 16, we plot the relative deviation of the actual values from their ideal values for different ENT tests. In this case also, the deviations increase with the increase of μTd .

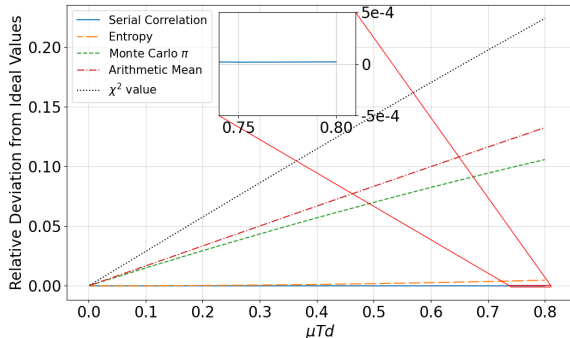


FIG. 16. Ent test result for the data simulated with the distribution given by Eq. (29). The relative deviation is calculated as $\frac{|v_i - v_o|}{v_i}$, where v_i is the expected ideal value for uniform distribution and v_o is the observed value for the simulated data. Although the deviation of the Monte Carlo value of π , the arithmetic mean and the χ^2 test value is high, the deviation of the entropy and the serial correlation is very small.

IX. DISCUSSION

In this article, we consider two perspectives for analyzing QRNG. From the manufacturer's point of view, we discuss how to determine when the source can be considered as quantum. Here we assume that photon detection time is available as a sample. We suggest two-fold statistical tests. The first one may be an interval estimation or hypothesis test to decide between sub-Poissonian and super-Poissonian. On the other hand, the last one, which is a χ^2 -test ensures Poisson distribution. This test can be performed for any quantum-photonic device to check its quantumness.

Then we discuss photon statistics for time-bin-based QRNG in practical scenarios. We consider two photon-arrival-time-based QRNG models, one using external time reference and another without such external reference. We show that, although for ideal devices these two models follow different distributions (one of which is perfectly random), these two QRNGs follow a similar distribution when the photon source is not an actual single photon source. We derive a relation when the photon statistics becomes ϵ -random. We found that by making the product of the expected number of photons (μT) within an external reference cycle (T) and the detection efficiency (d) small enough, the randomness of the generated raw random number can be increased. Therefore it would require less post-processing, and it would retain maximum randomness from the quantum source. This discussion would help QRNG manufacturers to design better QRNG.

Although small $\mu T d$ provides better randomness, from the user's perspective it may not be suitable. The random number generation rate, the timing error in registering photon detection time and the cost of the QRNG restrict us from choosing small values for μ , T or d . A

lower expected photon count improves quantumness but comes with increased costs and a reduced generation rate. On the other hand, a shorter external reference cycle enhances quantumness but must surpass a minimum threshold to reduce timing errors, having only slight effects on cost and rate. Reduced detection efficiency boosts quantumness and lowers costs, but also decreases the generation rate. The trade-off among the randomness sourced from quantum systems, the rate of random number generation, and the cost of the QRNG is contingent upon the specific requirements of the users.

Finally, we simulated random numbers according to the photon statistics we derived and applied statistical tests including NIST, Dieharder, AIS-31, and ENT to these numbers. The results from these tests validate our theoretical conclusions based on $\mu T d$ about the randomness of the quantum sources.

In practical cases, the dark count of a detector also contributes to the generation of random numbers. In our discussion, we did not consider the dark count. This work can be extended to see the effect of dark counts on the photon statistics. In our discussion, we have considered two models of photon arrival-time-based QRNGs. Similar analysis can be performed for other models of QRNGs.

One may note that our discussions are not meant for black-box testing for commercially available QRNGs. Rather, the physicists and engineers may use these in the QRNG design phase before post-processing, for evaluation, fine-tuning and performance optimization.

ACKNOWLEDGEMENT

S. Das would like to acknowledge the support received by the Quantum Delta NL KAT-2 project.

Appendix A: Relationship between Non-classicality of Light, antibunching of Photons and sub-Poissonian Distributions

The second-order correlation function [56] of light is defined by

$$g^2(\tau) := \frac{\langle I(t)I(t+\tau) \rangle}{\langle I(t) \rangle \langle I(t+\tau) \rangle}, \quad (\text{A1})$$

where $I(t)$ is the intensity of the light at time t and $\langle \cdot \rangle$ denotes the average over all t . Using the classical theory of light, it can be shown that

$$g^2(0) = \frac{\langle I(t)^2 \rangle}{\langle I(t) \rangle^2} \geq 1, \quad (\text{A2})$$

$$\text{and } g^2(\tau) = 1 \text{ for } \tau \gg \tau_c,$$

τ_c being the coherence time of the source.

Now, consider that a photon stream is sent through a beam splitter and two detectors D_0 and D_1 are kept in

two output paths. Than the correlation function (A1) can be written as

$$g^2(\tau) := \frac{\langle n_1(t)n_2(t+\tau) \rangle}{\langle n_1(t) \rangle \langle n_2(t+\tau) \rangle}, \quad (\text{A3})$$

where $n_i(t)$ is the number of counts registered on detector i at time t . If the incoming light consists of a photon stream with long intervals between two consecutive photons, the product $n_1(t)n_2(t)$ is always 0, giving $g^2(0) = 0 < 1$, which is not possible with classical lights. Thus, depending on $g^2(t)$, light is distinguished in the following three classes [56]:

- (i) bunched light, when $g^2(0) > 1$,
- (ii) coherent light, when $g^2(0) = 1$,
- (iii) antibunched light, when $g^2(0) < 1$.

Out of these three, antibunched light is undoubtedly non-classical.

The relation between photon count distribution and $g^2(\tau)$ is given by [55]

$$\langle (\Delta N)^2 \rangle - \langle N \rangle = \langle N \rangle^2 \frac{1}{T^2} \int_{-T}^T d\tau (T - |\tau|) (g^2(\tau) - 1). \quad (\text{A4})$$

In the above equation, if $g^2(\tau) \leq 1$ for all τ , it implies $\langle (\Delta n)^2 \rangle < \langle N \rangle$, i.e., a sub-Poissonian statistics, indicating non-classicality of light. However, if $g^2(\tau) \leq 1$ for some τ , there is no direct relation between the sub-Poissonian photon count statistic and the antibunching

of photons. Xou and Mandel [55] showed that if a source emits photons in two different nonvacuum modes, both having occupation number $n/2$, but different frequencies ω_1 and ω_2 , the second-order correlation function takes the form

$$g^2(\tau) = \frac{1}{2} \cos(\omega_1 - \omega_2)\tau - \frac{1}{n} + 1, \quad (\text{A5})$$

for $\tau < T$. Also, if $P(N, t, t+T)$ be the distribution of photon count in the time interval from t to $t+T$,

$$\langle (\Delta N)^2 \rangle - \langle N \rangle = \langle N \rangle^2 \left[\left(\frac{\sin(\omega_1 - \omega_2)T/2}{(\omega_1 - \omega_2)T/2} \right)^2 - \frac{1}{n} \right], \quad (\text{A6})$$

where $\langle N \rangle$ and $\langle (\Delta N)^2 \rangle$ are respectively the mean and the variance of the above distribution. Choosing $T = \frac{2\pi}{\omega_1 - \omega_2}$, it can be seen that $\langle (\Delta N)^2 \rangle < \langle N \rangle$, i.e., the light is sub-Poissonian although $g^2(0) = \frac{3}{2} - \frac{1}{n} > 1$ for $n > 2$ denoting the light is bunched. This example also shows that although both the antibunching of photons and the sub-Poissonian distribution of photon count indicate the non-classicality of light, they are not identical.

Appendix B: Quantum Entropy for QRNG

The Shannon entropy [86, 87] of the probability distribution given by Eq. (29) is given by

$$\begin{aligned} H(Q) &= - \sum_{i=1}^N f(i) \log f(i) \\ &= - \sum_{i=1}^N \frac{e^{\frac{\mu T d}{N}} - 1}{1 - e^{-\mu T d}} e^{-i \frac{\mu T d}{N}} \log \left(\frac{e^{\frac{\mu T d}{N}} - 1}{1 - e^{-\mu T d}} e^{-i \frac{\mu T d}{N}} \right) \\ &= - \frac{e^{\frac{\mu T d}{N}} - 1}{1 - e^{-\mu T d}} \sum_{i=1}^N e^{-i \frac{\mu T d}{N}} \left[\log \left(e^{-i \frac{\mu T d}{N}} \right) + \log \left(\frac{e^{\frac{\mu T d}{N}} - 1}{1 - e^{-\mu T d}} \right) \right] \\ &= \frac{e^{\frac{\mu T d}{N}} - 1}{1 - e^{-\mu T d}} \left[\log \left(e^{\frac{\mu T d}{N}} \right) \sum_{i=1}^N i e^{-i \frac{\mu T d}{N}} - \log \left(\frac{e^{\frac{\mu T d}{N}} - 1}{1 - e^{-\mu T d}} \right) \sum_{i=1}^N e^{-i \frac{\mu T d}{N}} \right] \\ &= \frac{e^{\frac{\mu T d}{N}} - 1}{1 - e^{-\mu T d}} \left[\log \left(e^{\frac{\mu T d}{N}} \right) \frac{e^{-\frac{\mu T d}{N}} \left[1 - (N+1)e^{-\mu T d} + N e^{-(N+1)\frac{\mu T d}{N}} \right]}{(1 - e^{-\frac{\mu T d}{N}})^2} - \log \left(\frac{e^{\frac{\mu T d}{N}} - 1}{1 - e^{-\mu T d}} \right) \frac{e^{-\frac{\mu T d}{N}} (1 - e^{-\mu T d})}{1 - e^{-\frac{\mu T d}{N}}} \right] \\ &= \frac{1 - (N+1)e^{-\mu T d} + N e^{-(N+1)\frac{\mu T d}{N}}}{(1 - e^{-\mu T d})(1 - e^{-\frac{\mu T d}{N}})} \log \left(e^{\frac{\mu T d}{N}} \right) - \log \left(\frac{e^{\frac{\mu T d}{N}} - 1}{1 - e^{-\mu T d}} \right). \end{aligned} \quad (\text{B1})$$

This is the entropy generated by the photon arrival-time-

based QRNGs we have discussed in this article.

- [1] J. Carlson, S. Gandolfi, F. Pederiva, S. C. Pieper, R. Schiavilla, K. E. Schmidt, and R. B. Wiringa, *Rev. Mod. Phys.* **87**, 1067 (2015).
- [2] N. Metropolis and S. Ulam, *Journal of the American Statistical Association* **44**, 335 (1949).
- [3] J. S. Bell, *Physics Physique Fizika* **1**, 195 (1964).
- [4] C. H. Bennett, G. Brassard, and A. K. Ekert, *Scientific American* **267**, 50 (1992).
- [5] C. E. Shannon, *The Bell System Technical Journal* **28**, 656 (1949).
- [6] E. Konstantinou, V. Liagkou, P. Spirakis, Y. C. Stamatiou, and M. Yung, in *Financial Cryptography*, edited by A. Juels (Springer Berlin Heidelberg, Berlin, Heidelberg, 2004) pp. 147–163.
- [7] K. Yamanaka and S.-i. Nakano, *IEICE TRANSACTIONS on Information and Systems* **100**, 444 (2017).
- [8] W. Schindler, “Random number generators for cryptographic applications,” in *Cryptographic Engineering*, edited by Ç. K. Koç (Springer US, Boston, MA, 2009) pp. 5–23.
- [9] M. Stipčević and Ç. K. Koç, “True random number generators,” in *Open Problems in Mathematics and Computational Science*, edited by Ç. K. Koç (Springer International Publishing, Cham, 2014) pp. 275–315.
- [10] X. Ma, X. Yuan, Z. Cao, B. Qi, and Z. Zhang, *npj Quantum Information* **2**, 1 (2016).
- [11] L. E. Bassham, A. L. Rukhin, J. Soto, J. R. Nechvatal, M. E. Smid, E. B. Barker, S. D. Leigh, M. Levenson, M. Vangel, D. L. Banks, N. A. Heckert, J. F. Dray, and S. Vo, *SP 800-22 Rev. 1a. A Statistical Test Suite for Random and Pseudorandom Number Generators for Cryptographic Applications*, Tech. Rep. (National Institute of Standards & Technology, Gaithersburg, MD, USA, 2010).
- [12] R. Brown, D. Eddelbuettel, and D. Bauer, *Dieharder: a random number test suite (version 3.31.1)*, Duke University Physics Department, Durham, NC 27708-0305 (2014).
- [13] W. Killmann and W. Schindler, “A proposal for: Functionality classes for random number generators,” (2011), AIS 20 / AIS 31 standard.
- [14] J. Walker, *ENT: a pseudorandom number sequence test program*, Fourmilab (2008).
- [15] M. Stipčević and B. M. Rogina, *Review of Scientific Instruments* **78**, 045104 (2007).
- [16] J. F. Dynes, Z. L. Yuan, A. W. Sharpe, and A. J. Shields, *Applied Physics Letters* **93**, 031109 (2008).
- [17] M. Wayne and P. Kwiat, *Optics express* **18**, 9351 (2010).
- [18] G. M. A. Michael A. Wayne, Evan R. Jeffrey and P. G. Kwiat, *Journal of Modern Optics* **56**, 516 (2009).
- [19] M. Wahl, M. Leifgen, M. Berlin, T. Röhlicke, H.-J. Rahn, and O. Benson, *Applied Physics Letters* **98**, 171105 (2011).
- [20] Y.-Q. Nie, H.-F. Zhang, Z. Zhang, J. Wang, X. Ma, J. Zhang, and J.-W. Pan, *Applied Physics Letters* **104**, 051110 (2014).
- [21] A. Khanmohammadi, R. Enne, M. Hofbauer, and H. Zimmermann, *IEEE Photonics Journal* **7**, 1 (2015).
- [22] Y. Zhang, H.-P. Lo, A. Mink, T. Ikuta, T. Honjo, H. Takesue, and W. J. Munro, *Nature communications* **12**, 1056 (2021).
- [23] R. Bernardo-Gavito, I. E. Bagci, J. Roberts, J. Sexton, B. Astbury, H. Shokeir, T. McGrath, Y. J. Noori, C. S. Woodhead, M. Missous, *et al.*, *Scientific reports* **7**, 17879 (2017).
- [24] K. Aungskunsiri, R. Amarit, K. Wongpanya, S. Jantarachote, W. Yamwong, S. Saiburee, S. Chanhorm, A. Intarapanich, and S. Sumriddetchajorn, *Applied Physics Letters* **119**, 074002 (2021).
- [25] C. Gabriel, C. Wittmann, D. Sych, R. Dong, W. Mauerer, U. L. Andersen, C. Marquardt, and G. Leuchs, *Nature Photonics* **4**, 711 (2010).
- [26] J. Y. Haw, S. M. Assad, A. M. Lance, N. H. Y. Ng, V. Sharma, P. K. Lam, and T. Symul, *Phys. Rev. Appl.* **3**, 054004 (2015).
- [27] X. Guo, C. Cheng, M. Wu, Q. Gao, P. Li, and Y. Guo, *Opt. Lett.* **44**, 5566 (2019).
- [28] Q. Zhou, R. Valivarthi, C. John, and W. Tittel, *Quantum Engineering* **1**, e8 (2019).
- [29] Z. Zheng, Y. Zhang, W. Huang, S. Yu, and H. Guo, *Review of Scientific Instruments* **90**, 043105 (2019).
- [30] T. Gehring, C. Lupo, A. Kordts, D. Solar Nikolic, N. Jain, T. Rydberg, T. B. Pedersen, S. Pirandola, and U. L. Andersen, *Nature Communications* **12**, 605 (2021).
- [31] B. Qi, Y.-M. Chi, H.-K. Lo, and L. Qian, *Opt. Lett.* **35**, 312 (2010).
- [32] H. Guo, W. Tang, Y. Liu, and W. Wei, *Phys. Rev. E* **81**, 051137 (2010).
- [33] Y. Shen, L. Tian, and H. Zou, *Phys. Rev. A* **81**, 063814 (2010).
- [34] F. Xu, B. Qi, X. Ma, H. Xu, H. Zheng, and H.-K. Lo, *Opt. Express* **20**, 12366 (2012).
- [35] Y.-Q. Nie, L. Huang, Y. Liu, F. Payne, J. Zhang, and J.-W. Pan, *Review of Scientific Instruments* **86**, 063105 (2015).
- [36] J. Yang, J. Liu, Q. Su, Z. Li, F. Fan, B. Xu, and H. Guo, *Opt. Express* **24**, 27475 (2016).
- [37] M. Huang, Z. Chen, Y. Zhang, and H. Guo, *Applied Sciences* **10**, 2431 (2020).
- [38] M. Herrero-Collantes and J. C. Garcia-Escartin, *Rev. Mod. Phys.* **89**, 015004 (2017).
- [39] V. Mannalatha, S. Mishra, and A. Pathak, *Quantum Information Processing* **22**, 439 (2023).
- [40] ID Quantique, “QUANTIS random number generator,” (2001).
- [41] Qutools, “quRNG|50 Quantum Random Number Generator,” (2010).
- [42] QNu Labs, “TROPOS Quantum Random Number Generator,” (2018).
- [43] Quintessence Labs, “qStream™ High-speed True Random Number Generation,” (2022).
- [44] Mars Innovation and Department of Electrical and Computer Engineering & Department of Physics, University of Toronto, “Quantoss high-speed quantum random number generator,” (2023).
- [45] Qantum Computing Inc., “uQRNG Uniform Probability Distribution Quantum Random Number Generator,” (2023).
- [46] Quside, “FMC series, PCIe series, QRNG security chipset,” (2023).
- [47] Qantum CTek, “Quantum Random Number Generator,” (2023).

- [48] C. Jones, J. Xavier, S. V. Kashanian, M. Nguyen, I. Aharonovich, and F. Vollmer, *Opt. Express* **31**, 10794 (2023).
- [49] J. Peřina, K. Thapliyal, O. Haderka, V. Michálek, and R. Machulka, *Optica Quantum* **2**, 148 (2024).
- [50] J. Peřina, K. Thapliyal, O. Haderka, V. Michálek, and R. Machulka, *Opt. Express* **32**, 537 (2024).
- [51] K. R. Bush and K. Børkje, *Phys. Rev. A* **109**, 043505 (2024).
- [52] L. Mandel, *Opt. Lett.* **4**, 205 (1979).
- [53] R. Alléaume, F. Treussart, J.-M. Courty, and J.-F. Roch, *New Journal of Physics* **6**, 85 (2004).
- [54] H. Paul, *Rev. Mod. Phys.* **54**, 1061 (1982).
- [55] X. T. Zou and L. Mandel, *Phys. Rev. A* **41**, 475 (1990).
- [56] A. Fox, *Quantum Optics: An Introduction*, Oxford Master Series in Physics (OUP Oxford, 2006) Chap. 5-6, pp. 75–125.
- [57] A. Imamoglu and Y. Yamamoto, *Phys. Rev. Lett.* **72**, 210 (1994).
- [58] J. Kim, O. Benson, H. Kan, and Y. Yamamoto, *Nature* **397**, 500 (1999).
- [59] C. Brunel, B. Lounis, P. Tamarat, and M. Orrit, *Phys. Rev. Lett.* **83**, 2722 (1999).
- [60] B. Lounis and W. E. Moerner, *Nature* **407**, 491 (2000).
- [61] C. Santori, M. Pelton, G. Solomon, Y. Dale, and Y. Yamamoto, *Phys. Rev. Lett.* **86**, 1502 (2001).
- [62] C. Santori, D. Fattal, J. Vučković, G. S. Solomon, and Y. Yamamoto, *Nature* **419**, 594 (2002).
- [63] J. Vučković, D. Fattal, C. Santori, G. S. Solomon, and Y. Yamamoto, *Applied Physics Letters* **82**, 3596 (2003).
- [64] A. Kuhn, M. Hennrich, and G. Rempe, *Phys. Rev. Lett.* **89**, 067901 (2002).
- [65] P. Adam and M. Mechler, *Optics Express* **32**, 17173 (2024).
- [66] S. Wang and M. Wang, *Applied Optics* **63**, 2608 (2024).
- [67] A. Kuznetsov, O. Nariezhnii, I. Stelnyk, T. Kokhanovska, O. Smirnov, and T. Kuznetsova, in *2019 10th IEEE International Conference on Intelligent Data Acquisition and Advanced Computing Systems: Technology and Applications (IDAACS)*, Vol. 2 (2019) pp. 713–717.
- [68] J. Park, S. Cho, T. Lim, S. Bhunia, and M. Tehranipoor, in *2019 IEEE/ACM International Conference on Computer-Aided Design (ICCAD)* (2019) pp. 1–8.
- [69] S. Chowdhury, A. Covic, R. Y. Acharya, S. Dupee, F. Ganji, and D. Forte, *Journal of Cryptographic Engineering*, **1** (2021).
- [70] L. Davidovich, *Rev. Mod. Phys.* **68**, 127 (1996).
- [71] T. K. Parařso, R. I. Woodward, D. G. Marangon, V. Lovic, Z. Yuan, and A. J. Shields, *Advanced Quantum Technologies* **4**, 2100062 (2021).
- [72] U. M. Titulaer and R. J. Glauber, *Phys. Rev.* **145**, 1041 (1966).
- [73] G. Casella and R. Berger, *Statistical Inference*, 2nd ed., Duxbury advanced series (Cengage Learning & Wadsworth, 2002) Chap. 8, pp. 373–413.
- [74] S. Ross, *Introduction to Probability and Statistics for Engineers and Scientists*, 4th ed. (Elsevier Science, 2009) Chap. 8, pp. 293–336.
- [75] R. Hogg and A. Craig, *Introduction to Mathematical Statistics*, 8th ed., Collier-Macmillan international editions (Macmillan, 2019) Chap. 4, pp. 225–315.
- [76] W. G. Cochran, *The Annals of Mathematical Statistics* **23**, 315 (1952).
- [77] F. J. Massey, *Journal of the American Statistical Association* **46**, 68 (1951).
- [78] T. W. Anderson and D. A. Darling, *The Annals of Mathematical Statistics* **23**, 193 (1952).
- [79] Y. Dodge, “Goodness of fit test,” in *The Concise Encyclopedia of Statistics* (Springer New York, New York, NY, 2008) pp. 233–234, 1st ed.
- [80] W. J. Conover, *Journal of the American Statistical Association* **67**, 591 (1972).
- [81] M. J. Slakter, *Journal of the American Statistical Association* **60**, 854 (1965).
- [82] C. Foreman, R. Yeung, and F. J. Curchod, “Statistical testing of random number generators and their improvement using randomness extraction,” (2024), preprint, arXiv:2403.18716 [cs.CR].
- [83] T. Jennewein, U. Achleitner, G. Weihs, H. Weinfurter, and A. Zeilinger, *Review of Scientific Instruments* **71**, 1675 (2000).
- [84] J. Argillander, A. Alarcón, C. Bao, C. Kuang, G. Lima, F. Gao, and G. B. Xavier, *Communications Physics* **6**, 157 (2023).
- [85] Y. Dodge, “Chi-square goodness of fit test,” in *The Concise Encyclopedia of Statistics* (Springer New York, New York, NY, 2008) pp. 72–76, 1st ed.
- [86] C. E. Shannon, *The Bell System Technical Journal* **27**, 379 (1948).
- [87] C. E. Shannon, *The Bell System Technical Journal* **27**, 623 (1948).